AGU PUBLICATIONS

Water Resources Research

RESEARCH ARTICLE
10.1002/2016WR019978

Key Points:
- Overall residence times of individual reservoirs ranged from 0.09 to 4.04 years
- Flow alteration by reservoirs range from 11 to 130%
- Secrecy maintained by developing countries in international rivers can be countered with satellite-based techniques

Correspondence to:
F. Hossain,
fhossain@uw.edu

Citation:
Bonnema, M., and F. Hossain (2017), Inferring reservoir operating patterns across the Mekong Basin using only space observations, *Water Resour. Res.*, *53*, 3791–3810, doi:10.1002/2016WR019978.

Received 20 OCT 2016
Accepted 18 APR 2017
Accepted article online 25 APR 2017
Published online 9 MAY 2017

Inferring reservoir operating patterns across the Mekong Basin using only space observations

Matthew Bonnema[1] and Faisal Hossain[1]

[1]Department of Civil and Environmental Engineering, University of Washington, Seattle, Washington, USA

Abstract This study explores the operating pattern of artificial reservoirs by examining their impact on streamflow through two parameters, residence time and flow alteration, using a purely satellite-based technique for the Mekong Basin. Overall residence times of individual reservoirs ranged from 0.09 to 4.04 years, while streamflow was altered between 11 and 130% of its natural variability. The current set of reservoirs appears to have increased the residence time of the entire Mekong basin by about 1 month. However, if subbasin variability is considered, the satellite-based method depicts a different picture. Residence time increases to 4 months when only regulated flows are considered. If low residence time reservoirs on major rivers are excluded and reservoirs on higher stream-order rivers considered, residence time increases to 1.3 years. Predictable strong seasonal patterns emerged in residence time, where reservoirs experience higher residence time in the dry season and lower residence time in the wet season and residence time varies inversely with precipitation. High variability in reservoir effects on streamflow between reservoirs could not be explained by any reservoir properties (e.g., size, use, location, etc.), highlighting the variability in the human decisions operating these reservoirs. The take-home message of this study is that satellite observations, in combination with physical models forced with satellite data, can elucidate the spatiotemporal variability of reservoir behavior in ungauged basins of the developing world. We demonstrate in this study that the requirement for ground data to monitor current or historical behavior of dams is not necessary.

Plain Language Summary The key take home message of our study is that satellites can now "see" the diverse variability of surface water residence time due to reservoir construction in ungauged and international river basins that is otherwise intractable. As satellite observations become increasingly more widespread in the near future, the scientific community will be able to rely on space observations to understand the potential impact of extensive reservoir development planned by each riparian nation of major river basins in the developing world. Such an ability will improve water management, inform planning decisions, and better reservoir operations. Such an understanding can also counter the secrecy or the lack of capacity that is common among nations, and result in a more cooperative environment for the benefit of all the stakeholders of the basin.

1. Introduction

Man-made reservoirs and dams provide tremendous societal benefits in the form of hydropower generation, flood control, irrigation, and water supply. However, by altering river flows and limiting transport of sediments, nutrients, and biota, these dams cause ecologically damaging impacts on the natural river system [*Ligon et al.*, 1995]. One study concluded that 25–30% of global sediment discharge is trapped within reservoirs annually [*Vörösmarty et al.*, 2003]. Numerous other studies have established links between dams and negative effects on the downstream ecosystem [*Pringle*, 2003; *Graf*, 2006]. Understanding how reservoirs are operated is key to elucidating reservoir impacts on hydrologic systems. Reservoir operations can be described by two linked parameters, storage and outflow, and how they change through time. This study demonstrates how such parameters can be used to inform stakeholders of reservoir impacts on river systems, focusing specifically on reservoir effects on streamflow by examining residence time and flow alteration.

Residence time, as defined in *Monsen et al.* [2002], is "how long a parcel, starting from a specified location within a waterbody will remain in the waterbody." For reservoirs, the specified starting location is typically

the point in which water enters the reservoir from upstream. The residence time of a reservoir is in essence, a measure of the time delay between when water enters the reservoir and when it is released by human operating decisions. Residence time controls biochemical processes such as nutrient accumulation and eutrophication processes [*Ambrosetti et al*., 2003] as well as sedimentation [*Kummu et al*., 2010] and fish population dynamics [*Beamesderfer et al*., 1990]. The residence time of a reservoir can be used to obtain first-order approximations of these and other complex processes, which dictate some impacts the reservoir has on the river system. In short, time-varying residence time can be considered as an important "piece of the puzzle" when attempting to reveal a reservoir's multifaceted impact on hydrology, geomorphology, and ecosystem function.

Flow alteration refers to the short-term effects of reservoir operation on downstream streamflow. That is, it is a measure of the instantaneous change in streamflow imposed by a reservoir. The degree to which flow is changed dictates the change in water supply the downstream population must manage. Altered river flows also impact ecosystem health and biodiversity [*Bunn and Arthington*, 2002]. While estimating the impact altered streamflows have on specific species is difficult, understanding the extent of reservoir imposed flow alteration is an important step in estimating these effects.

Unfortunately, in situ reservoir observations are largely unavailable, primarily in developing regions due to the inability of national agencies to routinely observe or the unwillingness of agencies to share the data openly. Such a situation has led many stakeholders to believe that reservoir behavior cannot be elucidated to the level required for making management decisions or long-term planning without actual in situ reservoir monitoring. This issue is made more urgent by the fact that dam construction in such regions is increasing [*Zarfl et al*., 2015].

With thousands of new dams planned for construction, it is imperative that the impacts of dams in these regions be more closely studied with or without in situ data. The situation pertinent to lack of in situ data is likely to persist or only worsen in future [*Gebregiorgis and Hossain*, 2014]. Thus, observations from space (i.e., satellite data) are the only viable alternative. Satellite remote sensing has been shown to have remarkable utility in observing reservoir operations [*Gao et al*., 2012; *McGuire et al*., 2006; *Allee and Johnson*, 1999; *Crétaux and Birkett*, 2006]. In a global analysis of reservoir flow alterations, *Döll et al*. [2009] states that the analysis could be refined if uncertainties related to reservoir operation rules could be limited. Hereafter, the terms "operation rules" and "operating policy" will be used interchangeably. Remotely sensed geophysical variables have the potential to provide the information necessary to understand reservoir operations in regions where few in situ data are available.

Past studies have characterized reservoir residence time as the volume of the reservoir divided by the mean annual inflow [*Vörösmarty et al*., 1997; *Kummu et al*., 2010; *Lehner et al*., 2011a, 2011b], which is more indicative of the design feature of a dam. This method also assumes of steady state conditions within the reservoirs, where volume remains constant and inflow is equal to outflow. This may be valid when studying long timescales, where annual inflow and outflow are equal. However, residence time can fluctuate greatly at shorter timescales due to variations in inflow, outflow, volume changes, and mixing processes [*Rueda et al*., 2006]. Accounting for this temporal variability in reservoirs requires observing these time-varying parameters.

Bonnema et al. [2016] used a combination of radar altimetry and Shuttle Radar and Topography Mission (SRTM) data to estimate the outflow of a reservoir in Bangladesh, which showed promise in providing the storage changes and outflows of reservoirs in ungauged basins. Furthermore, numerous studies also suggest that visible imaging missions such as Landsat can provide reasonable estimates of reservoir surface area [*Gao et al*., 2015; *Ji et al*., 2009; *Seeber et al*., 2010]. As we will show in this study, reservoir surface area is a key ingredient for deriving reservoir volume, which can be used to estimate outflow, flow alteration, and residence time.

The region of particular interest in this paper is the Mekong River Basin (MRB). The Mekong Basin is relatively underdeveloped in terms of river impoundments [*Kummu and Sarkula*, 2008]. There are approximately 46 dams in the basin, 3 of which are located on the main stem of the Mekong River in China [*Keskinen et al*., 2012; *Mekong River Commission (MRC)*, 2011]. As of 2012, there were 14 dams currently under construction, with another 78 planned [*Keskinen et al*., 2012; *MRC*, 2011]. Sixty million people live in the Lower Mekong Basin alone, and in some areas, up to 80% rely directly on the river for their food supply, primarily fish and floodplain agriculture. A Mekong River Commission (MRC) report finds that the planned main stem dams

would inflict USD 476 million/year of damages on fisheries within the river system, excluding any impacts on delta and coastal fisheries [*International Center for Environmental Management*, 2010]. Furthermore, these same dams are predicted to cause USD 25.1 million/year in lost agricultural land and USD 24 million/year in reduced nutrient loading to floodplain agriculture [*International Center for Environmental Management*, 2010]. While the mobility of fish also depends on reservoir design elements such as nature-like bypasses, the alteration of streamflow has been shown to consistently negatively impact fish health [*Schmutz and Mielach*, 2015; *Poff and Zimmerman*, 2010]. Understanding the impacts of these dams in greater detail is essential and begins with understanding the dams that currently exist in the basin. The operating patterns of reservoirs can reveal much about these multifaceted effects. Thus, the objective of this study is to estimate the temporal variations of residence time and flow alteration of current reservoirs in the MRB. This information could potentially be linked to existing hydrologic models of the basin, such as the MRC's Decision Support Framework (DSF), Variable Infiltration Capacity (VIC) model, Distributed Hydrology Soil Vegetation Model (DHSVM), or the MIKE Basin modeling suite, to provide key observations of reservoir impacts on the river system [*Johnston and Kummu*, 2012; *Adamson*, 2006; *Asian Development Bank (ADB)*, 2004; *Thanapakpawin et al*., 2007; *Costa-Cabral et al*., 2008].

Such a study can provide the foundation for studying reservoirs in other developing basins undergoing rapid change due to dam construction such as the Irrawaddy, Yangtze, Zambesi, Congo, or Amazon [*Winemiller et al*., 2016]. The benefit of a satellite-based approach is that it is unhindered by lack of availability of in situ data and has global applicability. Satellite-based reservoir technique can therefore be scaled regionally or globally to answer a diverse set of stakeholder and scientific community fundamental questions that have not been answered before. Some of these questions are: What are the impacts of dam operations on ecosystem services and flood risk in river basins? How are the impacts on regulated river systems likely to change in the future due to climate change, increasing development pressures and aggressive dam building plans by the developing world?

In the text that follows, section 2 describes the reservoirs studied here and provides an outline of the data available. Section 3 provides an overview of the method used to calculate residence time. Section 4 shows the results and provides discussion. Section 5 concludes with an overview and direction for future study.

2. Study Region

The MRB encompasses an area of 795,000 km^2 and spans six nations of China, Myanmar, Laos, Thailand, Cambodia, and Vietnam. It has an average annual discharge of 457 km^3. The basin experiences a tropical monsoon climate where a majority of the precipitation arrives from May through October, resulting in a similar seasonal pattern in streamflow. This study focused on the 20 large reservoirs identified by the Global Reservoir and Dam (GRanD) database [*Lehner et al*., 2011a, 2011b]. Figure 1 shows a map of the Mekong Basin with these 20 dams as well as future planned or under construction dams identified by *Zarfl et al*. [2015].

Table 1 lists the dam/reservoir name along with their capacity and degree of regulation (capacity volume divided by annual inflow volume), taken from the GRanD database. The capacity of these reservoirs ranges from 22.8 to 7030 $\times$ 10^6 m^3 with an average of 961 $\times$ 10^6 m^3. Degree of regulation (DOR) is the reservoir capacity expressed as a percentage of the mean annual inflow into the reservoir, which can be assumed as the "design" residence time of the reservoir.

For validation of the satellite-based technique, daily time series of in situ reservoir water levels was acquired for specific reservoir sites via our institutional agreement with Vietnam. In other cases, daily time series of reservoir volumes of some reservoir sites was acquired from publicly available websites (e.g., Thaiwater.net). Further validation was carried out on the Oroville Reservoir in California. This is outlined in greater detail in section 3.

3. Methodology

3.1. Residence Time

The key ingredients for estimating residence time are inflow (I), storage (S), and outflow (O). The driving concept behind the residence time calculation is that these terms obey a mass balance for every reservoir,

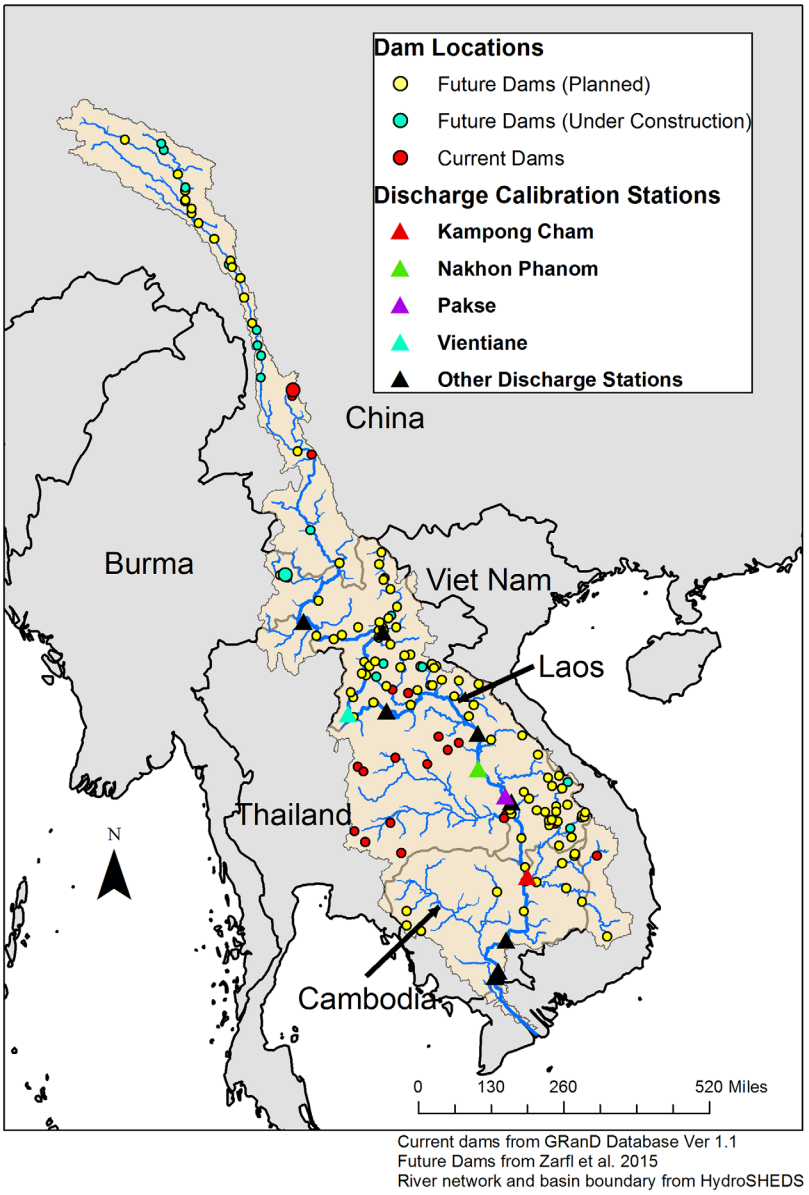

Figure 1. Map of Mekong River Basin with current and future dams, as well as the location of the in situ streamflow observations used to calibrate the VIC hydrologic model (section 3.3).

given by equation (1), where I is inflow, O is outflow, and ΔS is the change in storage over a duration of time.

$$O = I - \Delta S. \tag{1}$$

With the water in reservoirs obeying mass balance, several basic assumptions can be made in order to simplify the calculation of reservoir residence time:

1. A water parcel which enters the reservoir over a specific duration does not mix with other water parcels within the reservoir.
2. Water parcels exit the reservoir in order from oldest to newest.

Note that this is equivalent to assuming the reservoirs behave as plug flow reactors. With these two assumptions, the length of time a parcel of water spends in the reservoir can be identified. Generally speaking, a monthly time step was used, so the residence time of the inflow entering a reservoir during 1 month is the amount of time until

Table 1. List of Dams Examined in This Study and Their Capacities and Degrees of Regulation [*Lehner et al.*, 2011a, 2011b]

Dam/Reservoir Name	Capacity [million m^3]	Degree of Regulation (%)
Haixihai	61.9	197.7
Zibihe	93.2	131.6
Manwan	920	3.2
Nam Ngum	7030	87.5
Nam Leuk	185	72.3
Nam Oun	520	70.4
Nong Han Lake	1873.9	155.6
Nam Pung	165.5	102
Ubol Ratana	2263	83.2
Lam Pao	1430	48
Chulabhorn	188	198.1
Huai Kum	22.8	15.7
Lam Chang Han	26	156.4
Lamtakhong	310	189.8
Lamphraphloeng	152	86.7
Lamnangrong	150	161.6
Pak Mun	229	0.7
Sirindhorn	1966	142.7
Houayho	596	395.6
Yali	1037	17.1

all of the water is released that was in the reservoir just after the monthly inflow parcel arrived. This is expressed by equation (2), where t_0 denotes the time step of interest, $\theta(t_0)$ is the residence time of the water entering the reservoir at time t_0, and t_R is the time step in which the water that entered at time t_0 is released from the reservoir. This time of release is calculated by summing the amount of water exiting the reservoir in each time step, O(t), beginning at t_0 and ending when the sum is equal to the volume of the reservoir, $V(t_0)$ plus the amount of inflow, $I(t_0)$, at the time step of interest, t_0.

$$\begin{aligned}\theta(t_0) &= t_R - t_0 \\ I(t_0) + V(t_0) &= \sum_{t}^{t_R} O(t)\end{aligned}. \tag{2}$$

To average residence time of a single reservoir across time, an inflow weighted approach was used, as shown in equation (3).

$$\theta_{t-avg,r} = \frac{\sum_{t=1}^{T} I_{t,r}\theta_{t,r}}{\sum_{t=1}^{T} I_{t,r}}, \tag{3}$$

where $I_{t,r}$ is the inflow to reservoir r at time t, $\theta_{t,r}$ is the residence time of reservoir r at time t, and $\theta_{t\text{-}avg,r}$ is the time-averaged residence time of reservoir r over T time steps.

In order to estimate the collective effects of these reservoirs on the residence time of the basin as a whole, a similar averaging technique was used, shown in equation (4).

$$\theta_{b-avg} = \frac{\sum_{r=1}^{R}\left(\sum_{t=1}^{T} I_{t,r}\right)\theta_{t-avg,r}}{\sum_{t=1}^{R}\left(\sum_{t=1}^{T} I_{t,r}\right)}, \tag{4}$$

where $\theta_{b\text{-}avg}$ is the basin-average residence time over R reservoir and all other terms are as defined previously.

3.2. Flow Alteration

Reservoir imposed flow alteration (FA) is defined here as the percent difference between I and O. Substituting the mass balance between O, I, and ΔS (equation (1)) shows that this is equivalent to the ratio between ΔS and I, shown in equation (5).

$$FA = \frac{O-I}{I} = \frac{-\Delta S}{I}. \tag{5}$$

Note that positive FA indicates streamflow was increased by reservoir operations and negative FA indicates streamflow was decreased by reservoir operations. When averaging FA across longer timescales, the result should be close to 0, due to the principle of mass balance employed here. Thus, to derive meaningful information about a reservoir's overall effect on downstream flow, the absolute value of FA is used when averaging. This averaging process is inflow weighted, similarly to residence time, shown in equations (6) (time average) and (7) (basin average).

$$FA_{t-avg,r} = \frac{\sum_{t=1}^{T} I_{t,r}|FA_{t,r}|}{\sum_{t=1}^{T} I_{t,r}}, \tag{6}$$

$$FA_{b-avg} = \frac{\sum_{r=1}^{R}\left(\sum_{t=1}^{T} I_{t,r}\right) FA_{t-avg,r}}{\sum_{t=1}^{R}\left(\sum_{t=1}^{T} I_{t,r}\right)}, \quad (7)$$

where $FA_{t\text{-}avg,r}$ is the time-averaged flow alteration of reservoir r over T time steps, $FA_{r,t}$ is the flow alteration of reservoir r at time t, $FA_{b\text{-}avg}$ is the flow alteration, is the basin-average flow alteration over R reservoir and all other terms are as defined previously.

3.3. Reservoir Inflow

In order to estimate the inflow into each reservoir, a 0.1° resolution Variable Infiltration Capacity (VIC) Model of the MRB was employed [*Liang et al*., 1994]. The model was constructed using land cover data from the Global Land Cover Characterization (GLCC) data set and soil data prepared by the Harmonized World Soil Database (HWSD) [*Loveland et al*., 2000; *FAO/IIASA/ISRIC/ISSCAS/JRC*, 2012]. Monthly leaf area index and albedo were provided by the Moderate Resolution Imaging Spectroradiometer (MODIS) mission and topography information was obtained from SRTM. The meteorological forcings such as temperature (minimum and maximum), wind speed, and precipitation were obtained from 237 weather station records archived as Global Summary of the Day (GSOD) by National Climatic Data Center (NCDC). This model was calibrated using streamflow observations from 13 in situ gage stations from 2003 to 2008. Validation of the calibrated model with data from the same gage stations from 2009 to 2013 resulted in model bias ranging from −17.8 to 27.1% (Table 2). Figure 2 shows the fit of the calibration and validation for four of these stations, corresponding to the error statistics shown in Table 2.

This model was run at the daily time step from 2002 through 2015 (14 years), providing surface water fluxes for each 0.1° grid cell. These modeled fluxes were then regridded to 0.01° resolution, because 0.1° cells did not properly resolve the correct stream channels feeding into the reservoirs. The regridding was performed by assigning all 0.01° cells the value of the 0.1° cell containing them. These fluxes were then run through a streamflow routing model of the basin to obtain daily inflow into each reservoir [*Lohmann et al*., 1996]. The regridding was necessary to simulate reservoir inflow at the appropriate resolution because some of the reservoirs are built on smaller rivers that would not appear in 0.1° resolution topography. The routing model used estimates of surface runoff from the VIC model and routed this water to river channels according to input topographical information. The daily flows were then aggregated into average monthly inflow. Figure 3 (top) shows monthly averaged basin precipitation and basin outflow at the MRB delta (i.e., the basin outlet), averaged across the entire 2002 through 2015 time period. Precipitation and outflow are both seen to increase from May through September, decrease from September through December, and then remain stably low from January through April. This pattern is fairly representative of the local inflow behavior at each reservoir, with the exception that lag between precipitation and inflow being much shorter than 1–2

Table 2. VIC Model Calibration Error Statistics[a]

Basin	Category	Bias (%)	NRMSE (%)	Efficiency	Correlation
Chiang Sean	Base	−52.6	70.6	0.64	0.80
	Calibration	−6.3	35.5	0.80	0.90
	Validation	8.6	42.5	0.57	0.87
Luang Prabang	Base	−37.2	63.1	0.69	0.84
	Calibration	6.6	37.5	0.84	0.92
	Validation	27.1	52.8	0.70	0.92
Vientiane	Base	−42.5	63.3	0.71	0.84
	Calibration	−4.8	35.3	0.84	0.92
	Validation	15.3	41.3	0.78	0.92
Nakhon Phanom	Base	−21.1	63.3	0.71	0.84
	Calibration	−29.3	52.4	0.78	0.93
	Validation	−17.8	36.3	0.88	0.95
Pakse	Base	−18.6	63.3	0.71	0.84
	Calibration	−3.2	38.7	0.86	0.93
	Validation	8.0	34.2	0.89	0.95
Kampong Cham	Base	−12.9	63.3	0.71	0.84
	Calibration	−16.7	45.3	0.84	0.93
	Validation	−4.3	40.9	0.85	0.92

[a]Base represents the uncalibrated model performance for 2003–2008, calibration represents the performance of the calibrated model during the calibration period (2003–2008), and validation represents calibrated model performance from 2009 to 2013.

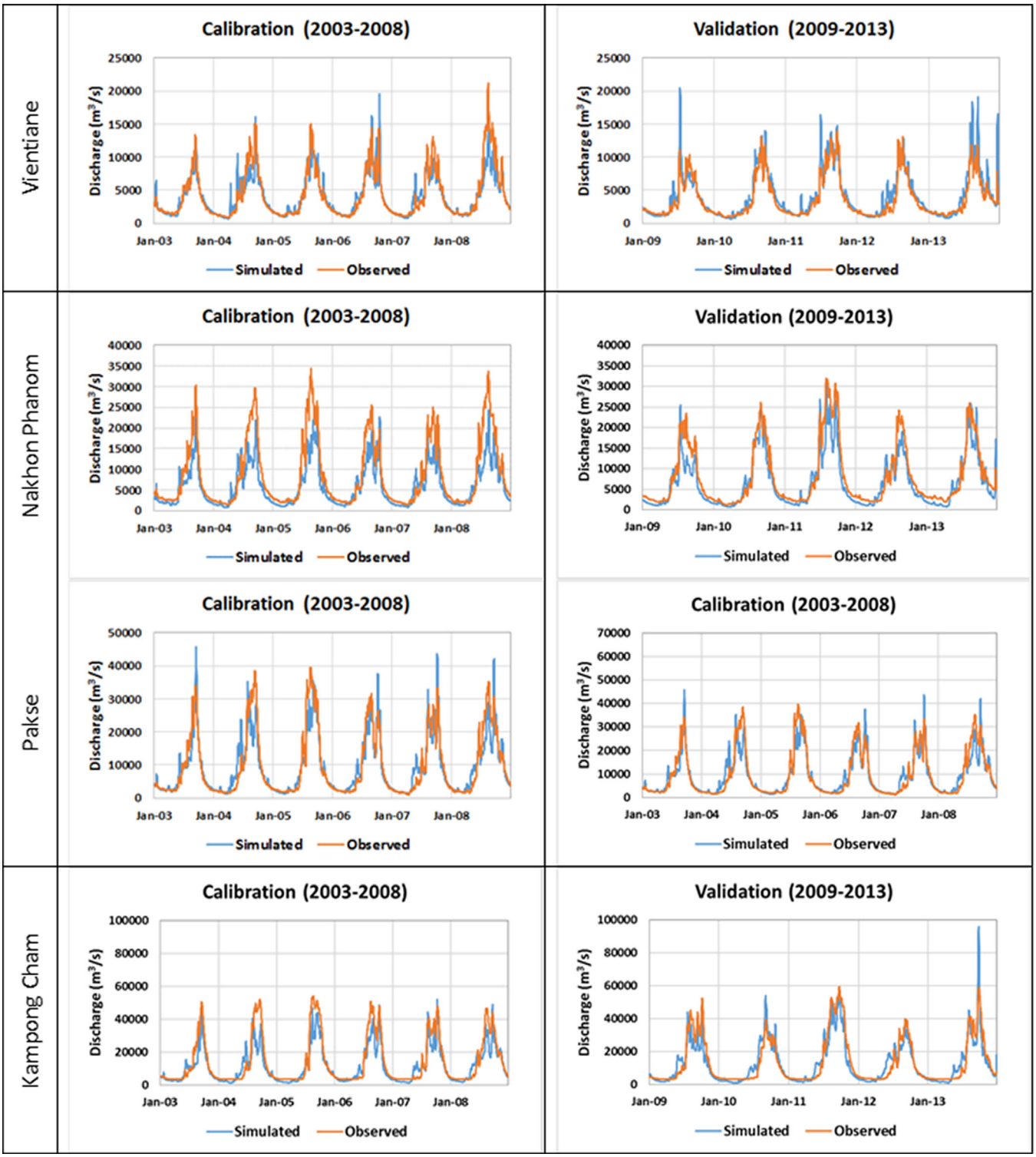

Figure 2. Calibration and validation of VIC model at four selected streamflow gaging stations on the main stem of the Mekong River. Note: the calibration and validation was carried out at all the streamflow locations shown in Figure 1, but only samples of four locations are shown herein.

months for smaller basins. Figure 3 (bottom) shows the annual average basin precipitation and basin outflow from 2002 through 2015. A point to note is that the VIC model represents natural streamflows and does not take the effects of reservoir operations into account. Therefore, the inflow of reservoirs

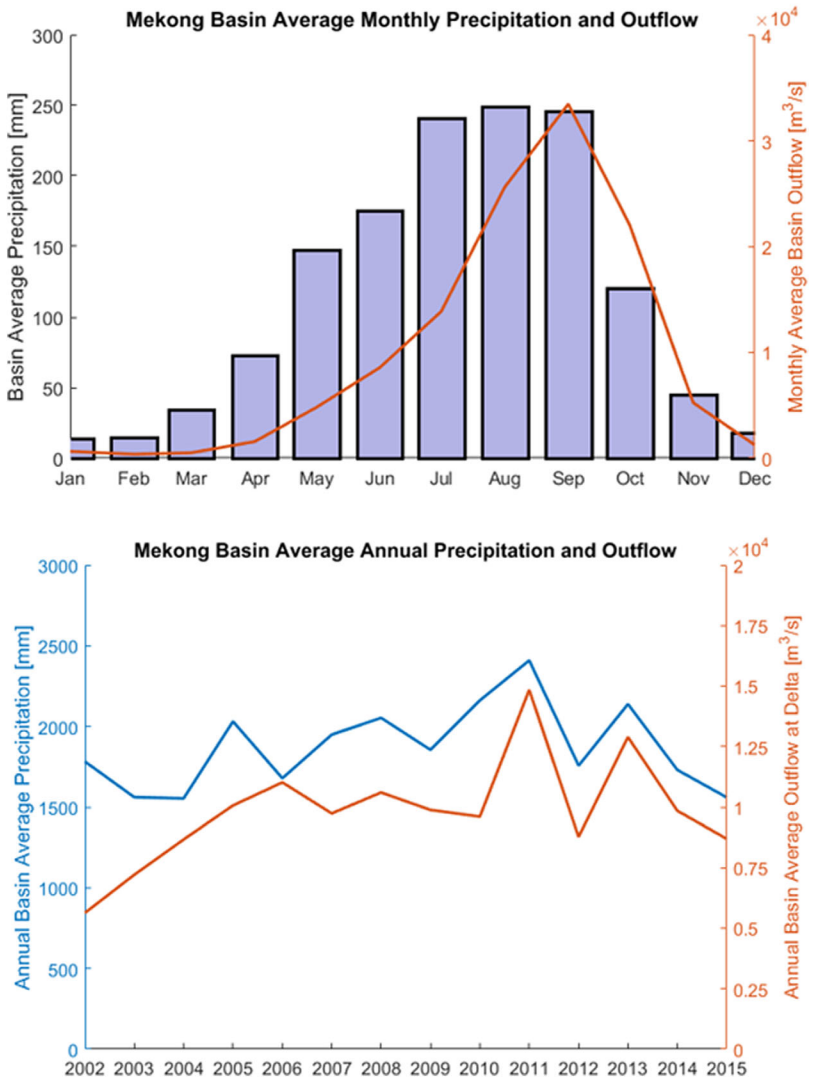

Figure 3. Monthly averaged basin precipitation and outflow at the MRB delta from VIC model (top) and annual average basin precipitation and outflow at delta from 2002 through 2015 from VIC model (bottom).

downstream of other reservoirs was adjusted according the outflow of each upstream reservoir (discussed in greater detail in section 3.4).

3.4. Reservoir Storage

The estimation of reservoir storage was a three-step process. First, a relationship between reservoir surface area and elevation was established for each reservoir. This relationship is known as the area-elevation curve. Next, the area-elevation curve was used to convert satellite measurements of either water surface elevation or surface area into reservoir volume (known as the area-volume curve). Finally, a monthly operations curve (i.e., operating policy) was established from a long record of satellite observations and used to fill gaps in the satellite record. Each of these processes is described in greater detail below.

3.4.1. Area-Elevation Curve

The method used here is similar to the method employed in *Bonnema et al*. [2016]. For each reservoir, a 30 m resolution digital elevation model (DEM) provided by the Shuttle Radar and Topography Mission (SRTM) was classified into 1 m elevation bands over the reservoir and surrounding area. The surface area of each band provides an estimate of the reservoir surface when water reaches that elevation. This provided information on the bathymetry of the reservoir above the elevation of the water at the time of the SRTM observation (i.e., February 2000). To estimate the bathymetry below this elevation, a power curve was fitted to the lowest observed elevation bands and extended below the water surface. This curve is

used to extrapolate the curve to capture the bathymetry below the level the water was at when SRTM observed the reservoir.

3.4.2. Reservoir Volume

The volume of a reservoir is then computed using either radar altimetry-based water surface elevations or spectral (visible) band-based water surface area from Landsat. The Sirindhorn Reservoir is the only reservoir of the 20 examined here that is observed by a satellite altimeter. For this reservoir, elevations obtained from the Jason-2 satellite altimetry mission were used. Using the area-elevation curve, the reservoir surface area corresponding to the observed elevation was identified. For all other reservoirs, Landsat images were used to estimate reservoir surface area. Specifically, the normalized difference water index (NDWI) was used to classify water pixels from 30 m resolution Landsat spectral images [*McFeeters*, 1996]. This method identifies which pixels of a Landsat image likely contain water by calculating the NDWI for each pixel, according to equation (8),

$$NDWI = \frac{X_{green} - X_{nir}}{X_{green} + X_{nir}}, \tag{8}$$

where X_{green} and X_{nir} are the reflectance values in the green and near infrared wavelengths, respectively. The green wavelength corresponds to Band 3 from Landsat 8 and Band 2 from Landsat 4, 5, and 7. The near-infrared wavelength corresponds to Band 5 from Landsat 8 and Band 4 from Landsat 4, 5, and 7. Pixels with NDWI greater than 0 were classified as water pixels and pixels with NDWI less than 0 were assumed to not contain surface water [*McFeeters*, 1996]. The surface area of the water pixels is then the estimate of the reservoir surface area at the time of the Landsat overpass. Again, using the area-elevation curve, the corresponding water surface elevation was identified.

With both water elevation and surface area known, the volume of the reservoir can be computed by estimating the volume of water required to fill the reservoir to the storage capacity listed in the GRanD database [*Gao et al.*, 2012]. This is done using a trapezoidal approximation (equation (9)), where V is the volume of the reservoir, A is the reservoir surface area, h is the reservoir elevation, and the subscript c denotes these quantities at reservoir capacity.

$$V = V_c - (A_c + A)(h_c - h)/2. \tag{9}$$

3.4.3. Reservoir Operations Curve

A significant issue with building a time series of reservoir surface areas with Landsat images is the potential for unusable images due to cloud cover, which can lead to long temporal gaps in data. This was overcome here by employing a method similar to the approach outlined in *Yoon and Beighley* [2015]. Here the assumption is made that reservoirs are operated at a relatively stable level on a submonthly scale and when looked over a long record, variability of reservoir operation at submonthly scales remains within a narrow range. This is a fairly realistic assumption as most reservoirs strive to follow the rule curve and make release and storage decisions according to a predefined standard operating procedure (SOP).

The reservoir volumes estimated from the entire record of Landsat images were thus grouped by month and the average reservoir volume for each month was calculated. This formed an approximation of the reservoir operations curve. This process is illustrated by Figure 4. The utilization of green and NIR Landsat bands to estimate water surface is depicted in the top figures and the derivation of the area-elevation curve is shown in the bottom left figure. A single water surface area estimate, when paired with the area-elevation curve, led to a single point on the operations curve in the bottom right figure. With a long record of Landsat images, the average reservoir volume for each month can be estimated. This monthly average is the approximation of the operations curve, which was then used to fill gaps in the time series of reservoir volume generated from Landsat images. For each monthly time step where no cloudless Landsat image exists, reservoir volume from the approximated operations curve was used. The operations curve was completely disregarded in favor of Landsat-based volume estimates, when available. Figure 5 shows the fraction of months without any usable Landsat images from 2002 through 2015, averaged across all reservoirs, as well as the range of unobserved months of all reservoirs. Unsurprisingly, the months with the least amount of usable Landsat images occur when precipitation is the highest (see Figure 3).

3.5. Reservoir Outflow

Reservoir outflow was estimated using the same mass balance described earlier by equation (1) [*Bonnema et al.*, 2016]. This method has been shown to provide accurate reservoir outflow estimates at monthly

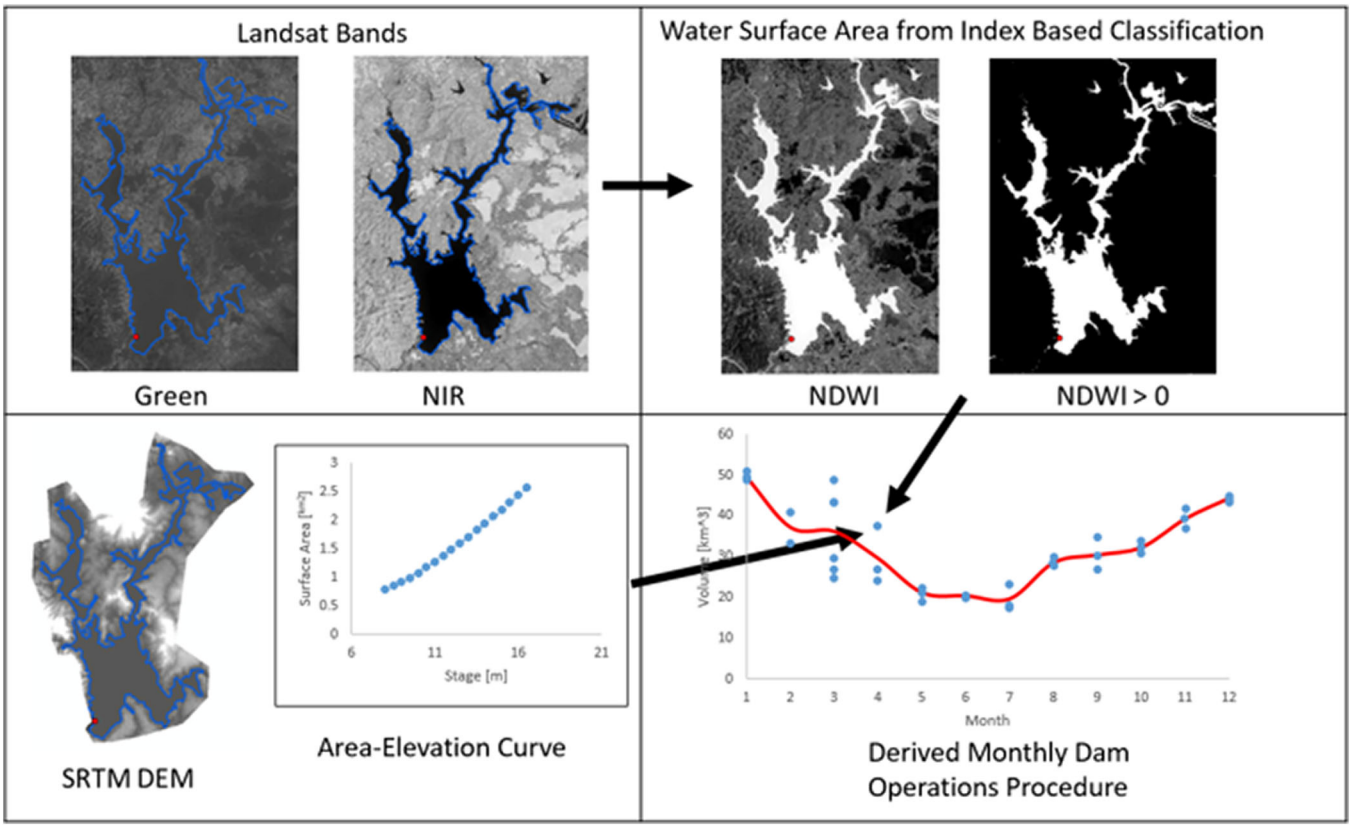

Figure 4. Flowchart depicting process of approximating reservoir operations curve. (top left) The green and NIR Landsat bands. (top right) The Normalized Difference Water Index (NDWI) and the classified water pixels. (bottom left) An area-elevation curve and the SRTM 30 m DEM it was derived from. (bottom right) The derived operations curve (monthly averages of reservoir volume). A single point on the curve is the result of the combination of one NDWI classified image with the area-elevation curve.

timescales for the Kaptai Reservoir in Bangladesh, which is located in a similar tropical monsoon climate as the MRB [*Bonnema et al*., 2016]. Based on the results of this past study, evaporation was neglected from the mass balance.

As previously stated, these outflows were used to correct the inflows of downstream reservoirs. Since the routing model conserves water in the river network, the downstream inflows are adjusted by the amount of

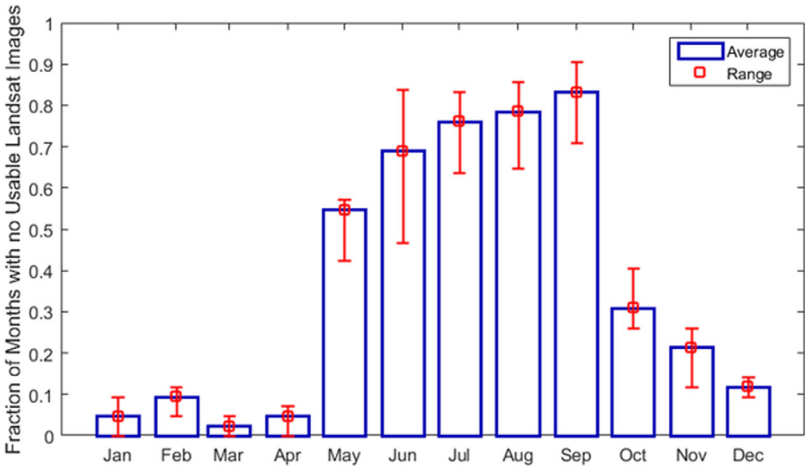

Figure 5. Average and range of fractions of months with usable Landsat observations, by month over the 14 year period.

total storage change in upstream reservoirs (equation (5)) where I_{adj} is the adjusted inflow, I is the natural inflow (modeled by VIC), and ΔS_{up} is the storage change of upstream reservoirs.

$$I_{adj} = I - \sum \Delta S_{up}. \tag{10}$$

4. Results and Discussion

4.1. Validation of Satellite-Based Volume Estimates

There are several limitations in the satellite-based approach employed here, such as long sampling frequency (relative to ground-based approaches), interference from clouds and other atmospheric effects, and uncertainties associated with deriving water surface area from spectral data. Thus, validating these methods to ground-based measurements is essential. Figure 6 (top) shows reservoir volumes estimated by ground

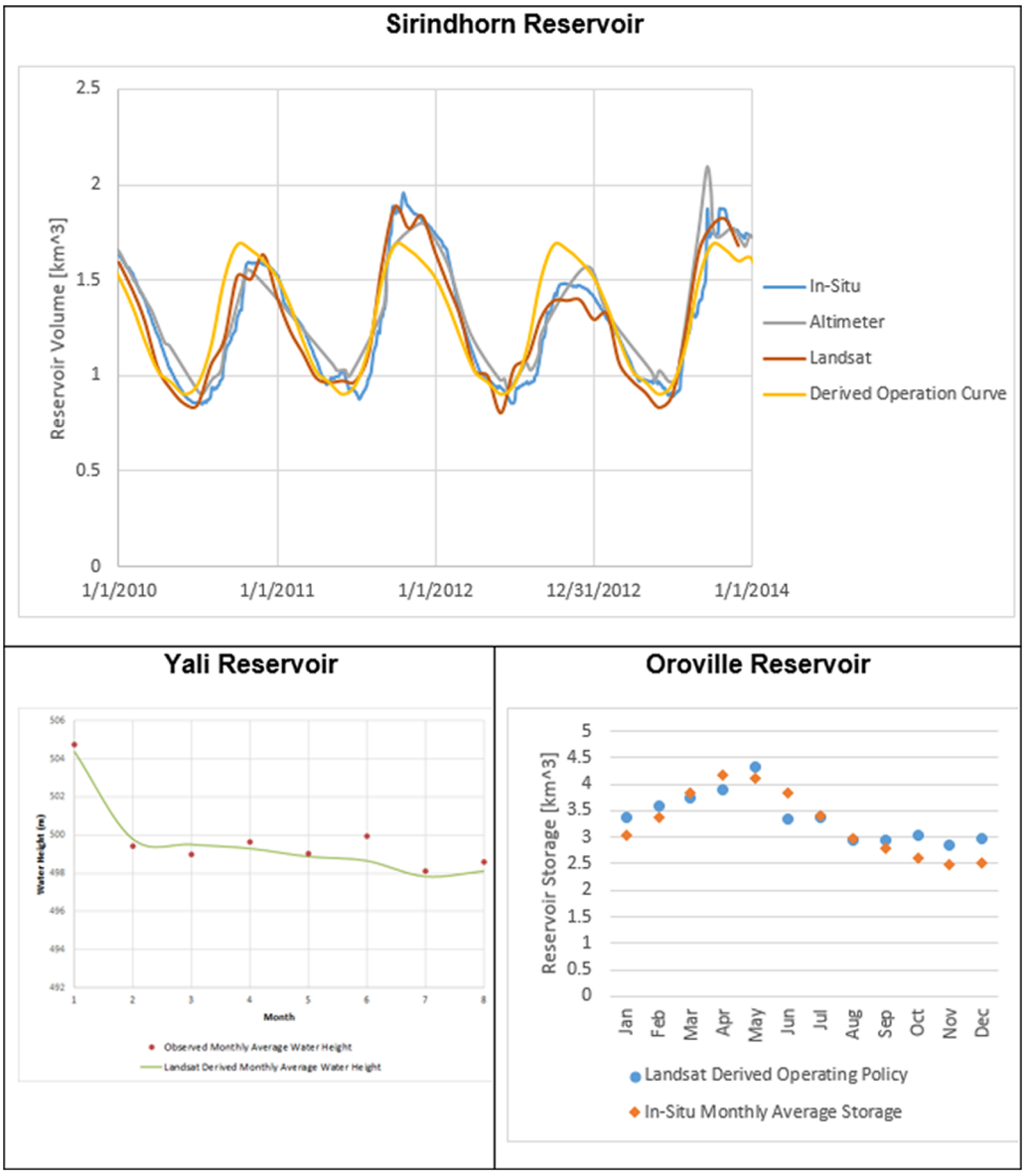

Figure 6. (top) Comparison between ground observed, altimeter derived, Landsat derived, and approximated operating policy estimated reservoir volume for the Sirindhorn Reservoir, (bottom left) comparison between observed monthly average water height and Landsat-derived water height for the Yali Reservoir for 8 months in 2016, and (bottom right) comparison between Landsat-derived operating policy and in situ monthly average storage of the Oroville Reservoir.

observations (in situ), altimeter water height data, Landsat surface area, and derived operations curve for the Sirindhorn Reservoir. Comparison between the altimeter and in situ volumes and taking the ground observed value as the true volume results in a root mean squared error (RMSE) of 0.27 km^3, which is 19% of the average reservoir volume in this time period. Similarly, comparisons between the Landsat and in situ volumes agree to within 20% of RRMSE. This indicates that the altimetry and Landsat-based methods of estimating reservoir volume are both successful (within a 20% error range) in capturing the month-to-month reservoir volume fluctuations. Furthermore, when the in situ observations were used to estimate residence time, the resulting residence times agreed with altimeter and Landsat-derived residence times to within 15 and 17% RRMSE, respectively.

Due to the linear relationship between flow alteration and storage, a 19% RRMSE in altimeter-based volume results in 19% RRMSE in FA and 20% RRMSE in Landsat volume results in 20% RRMSE in FA. Comparison between volumes estimated from the derived monthly operations curve and the in situ resulted in 32% error. While this is substantially worse than Landsat or altimeter methods, it is important to note that this method is only employed at times when Landsat data are unavailable, primarily occurring during the wet season. Based on the results from the Sirindhorn Reservoir, this would result in overestimations of storage during wet seasons. Such overestimations would lead to underestimations of wet season outflows, potentially increasing flow alteration and leading to longer residence times. Subsequently, overestimations of wet season storage would increase flows during the transition from wet to dry season, which would decrease flow alteration and residence time.

Unfortunately, the Sirindhorn Reservoir is the only reservoir studied here that was overpassed by a satellite altimeter to provide skillful height variations. Nevertheless, the close agreement between satellite-based volume and the in situ volume established a good level of trustworthiness in our comprehensive satellite-based approach that synthesizes multiple platforms for other reservoirs of the MRB. Figure 6 (bottom left) compares the actual monthly water level elevations of the Yali Reservoir to elevations derived from the visible Landsat images. This Landsat-derived water surface elevations exhibit an RMSE of 0.57 m, which is 8.6% of the range in actual water surface elevations observed during this time period. Figure 6 (bottom right) shows a comparison between a Landsat-derived operations curve and the average monthly volume of the Oroville reservoir from 2010 to 2016. These two monthly averaged volumes agree to within 17% RRMSE and compares well with the well-known design rule curve of Oroville dam. Overall, these results signify that both the Landsat-based method and the altimeter-based method are certainly capable of accurately estimating water surface heights and consequential volume changes. These results also demonstrate the skill of average operating policy estimation and its usefulness to estimate volume when no other sources of data are available.

4.2. Reservoir Residence Time and Flow Alteration

Figure 7 shows the average and range of the estimated reservoir operations curves, normalized by their maximum storage so that comparisons can be made between reservoirs of different volumes. While there is

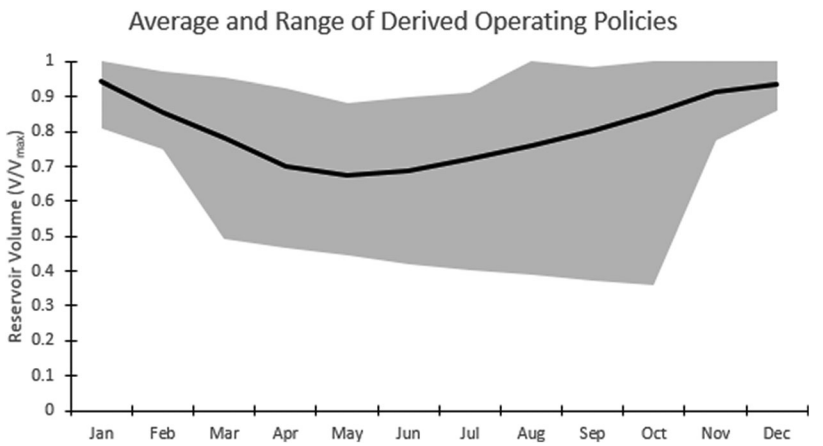

Figure 7. Average and range of derived reservoir operations curves (i.e., "effective") for all reservoirs, normalized by reservoir maximum volume. Average shown in black.

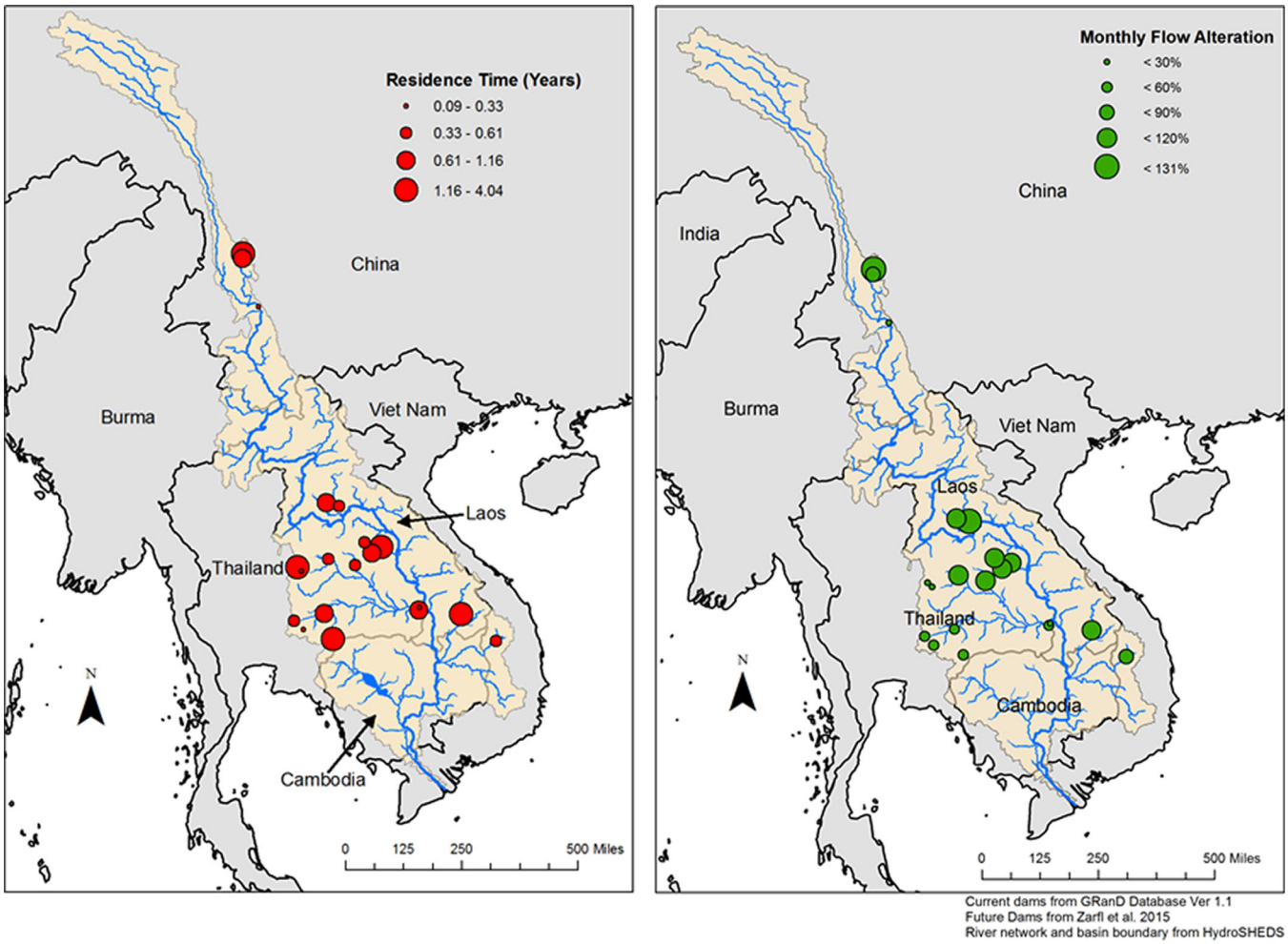

Figure 8. Map displaying the residence time (left) and flow alteration (right) of reservoirs in the Mekong Basin.

variation among the different reservoirs, as evident by the large range, a dominant trend can be gleaned, of higher volume at the beginning of the dry season, followed by decline into the wet season. At the end of the wet season, the reservoirs fill again. This trend is highlighted by the average normalized operations curve which is shown in black.

Figure 8 displays how the resulting residence times are distributed throughout the MRB. Figure 8 also shows the resulting average absolute flow alterations for each reservoir in the MRB. These residence time and FA values are also shown in Table 3 broken down as a function of season: wet season (June through October) and the dry season (November through May). Residence times ranged from 0.09 to 4.04 years and FA ranged from 11 to 131%. Note that the overall average FA is the average of the magnitudes of monthly FA, while the wet and dry season FA preserved the sign, in an attempt to characterize the nature of the flow alterations. FA was largely negative in the wet season and positive in the dry season, reinforcing the trend exhibited by the operations curves. Reservoirs with low residence time also exhibited low FA.

Figure 9 shows a comparison between the residence time estimated in this study and the DOR estimated in the GRanD database. DOR was estimated in *Lehner et al.* [2011a, 2011b] by dividing reservoir capacity by long-term average annual inflow. It should be noted that the time frame from which this average annual inflow represents is different from the time frame examined in this study. DOR is essentially the reservoir capacity expressed as a percentage of the annual average inflow and is similar to residence time, as calculated using a similar method than the one employed here. Thus, it is a good point of comparison for the resulting residence times from this study. Figure 9 presents DOR as the number of years of inflow which can be stored within a reservoir. This figure shows some agreement between the simple to obtain DOR and the

Table 3. Estimated Overall and Seasonal Residence Time and Flow Alteration for Each Reservoir

Dam Name	Overall Residence Time (Year)	Dry Season Residence Time (Year)	Wet Season Residence Time (Year)	Overall Absolute FA (%)	Dry Season FA (%)	Wet Season FA (%)
Haixihai	2.07	2.08	2.05	131.0	142.6	−81.1
Zibihe	1.15	1.15	1.13	72.6	65.9	−26.5
Manwan	0.12	0.18	0.07	17.2	16.2	
Nam Ngum	1.16	1.18	1.15	108.2	56.3	−36.3
Nam Leuk	0.58	0.59	0.45	125.4	114.1	−96.1
Nam Oun	0.61	0.63	0.57	99.2	103.5	−58.0
Nong Han Lake	2.33	2.35	2.32	118.2	1.6	−31.0
Nam Pung	0.95	1.05	0.93	106.9	7.5	−31.6
Ubol Ratana	0.56	0.61	0.50	112.3	25.5	−24.6
Lam Pao	0.53	0.53	0.43	101.9	47.8	−21.6
Chulabhorn	2.08	2.09	2.05	26.2	40.1	−4.1
Huai Kum	0.22	0.30	0.21	11.1	20.6	−0.05
Lam Chang Han	0.89	0.92	0.84	39.3	57.3	−2.1
Lamtakhong	0.58	0.59	0.49	50.8	24.2	−5.4
Lamphraphloeng	0.33	0.33	0.33	57.1	3.9	−0.05
Lamnangrong	1.94	1.96	1.93	48.5	21.7	−4.7
Pak Mun	0.09	0.25	0.06	11.5	12.3	−1.2
Sirindhorn	0.96	1.04	0.91	58.4	61.7	−15.4
Houayho	4.04	4.05	3.98	99.7	15.6	−4.6
Yali	0.44	0.66	0.38	74.6	10.4	−18.5

temporally varying approach employed here; however, other reservoirs show significant differences. No correlation between the capacity, stream order, or reservoir use could be established that would explain this difference, although a larger sample size of reservoirs could provide greater clarity.

4.2.1. Temporal Variations

As seen in Table 3, residence time was typically larger during dry season than wet season. This agrees with what is known about seasonal variations in streamflow and reservoir operations. Figure 7 illustrates the typical seasonal trend observed in reservoir volume, where reservoirs are kept low during the start of the wet season and allowed to fill toward the end of the wet season. This is followed by high reservoir volume in the beginning of the dry season, as reservoirs are then being used to store water and release it in a controlled fashion throughout the wet season. The low inflows in the dry season led to a decrease as water is discharged for irrigation, water supply, or hydropower generation. It is this long, slow release of water in the dry season that causes residence time to increase. Similarly, the rapid outflows and lower volume combined

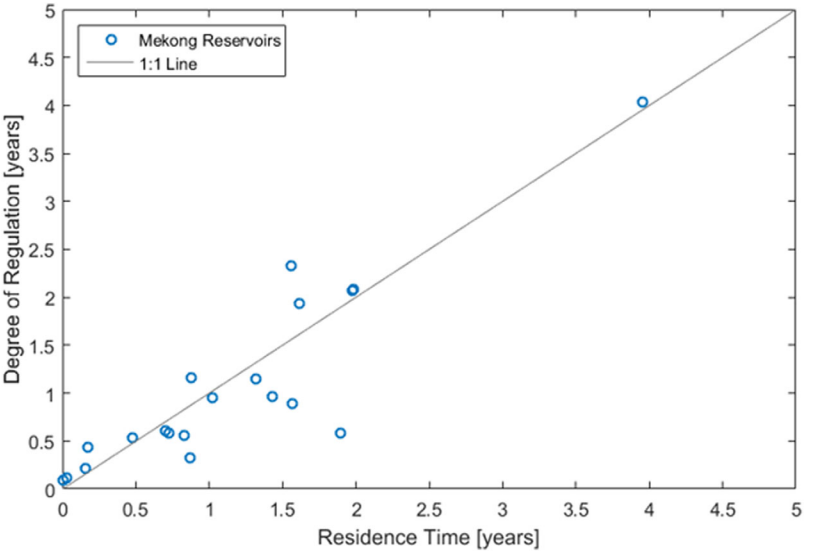

Figure 9. Comparison between residence time estimated in this study and degree of regulation (DOR) from the GRanD database. Here DOR is the reservoir capacity expressed in years of average annual inflow. 1:1 line shown in gray.

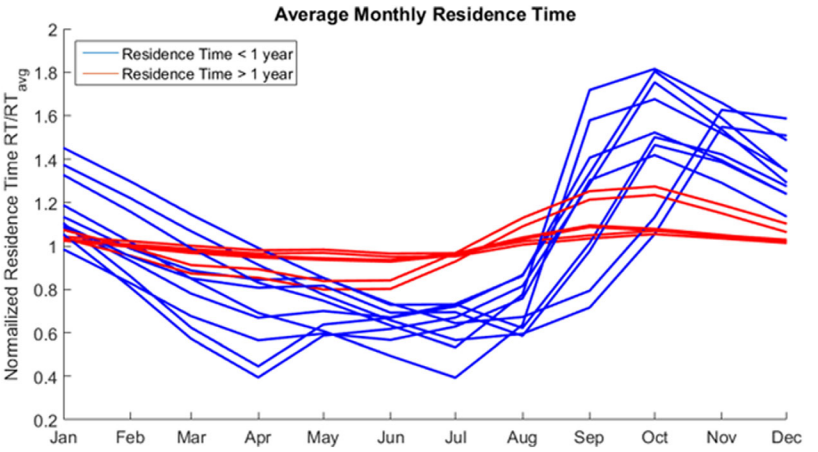

Figure 10. Average monthly residence time for each reservoir, normalized by each reservoir's average residence time. Reservoirs with residence time less than 1 year are shown in blue. Reservoirs with residence time greater than 1 year are shown in red.

in the wet season lead to lower residence time. Figure 10 plots the average monthly residence time of all reservoirs, each normalized by the reservoir's average residence time. This plot further elucidates the seasonal trend in residence time.

It also reveals that reservoirs with higher average residence time exhibit less seasonal fluctuation in residence time (reservoirs with residence time greater than 1 year are shown in red in Figure 10). Similarly, reservoirs with lower average residence time have more pronounced seasonal variations than reservoirs with higher residence time. A likely explanation for this pattern is that these reservoirs in the MRB with higher average residence time tend to have higher storage capacity relative to their inflow. This indicates that such reservoirs would be inherently less sensitive to fluctuations in inflow, resulting in a more consistent residence time. For example, water entering the Houayho Reservoir is estimated to stay within the reservoir for approximately 4 years before being released. This water resides in the reservoir over the course of multiple wet and dry seasons, dampening the seasonal trend described earlier. In contrast, water entering the Sirindhorn Reservoir is only estimated to stay in the reservoir just under 1 year, resulting in single seasons or months have more of an effect on residence time.

Figure 11 shows the yearly average residence time for each reservoir from 2002 through 2015, grouped by average residence time. Note that since the method employed here estimates residence time by following

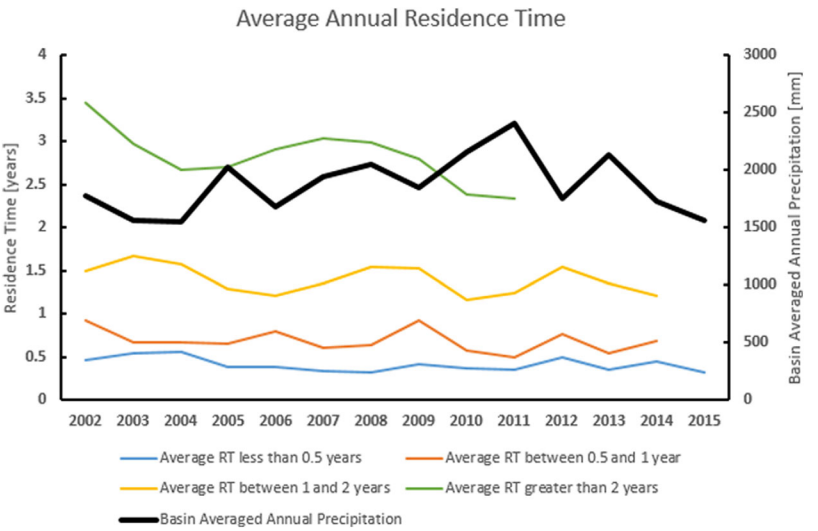

Figure 11. Average annual residence time, grouped by residence time ranges and plotted with basin-averaged annual precipitation. Each colored line represents the average annual residence time of all reservoirs with average overall residence time within the listed range.

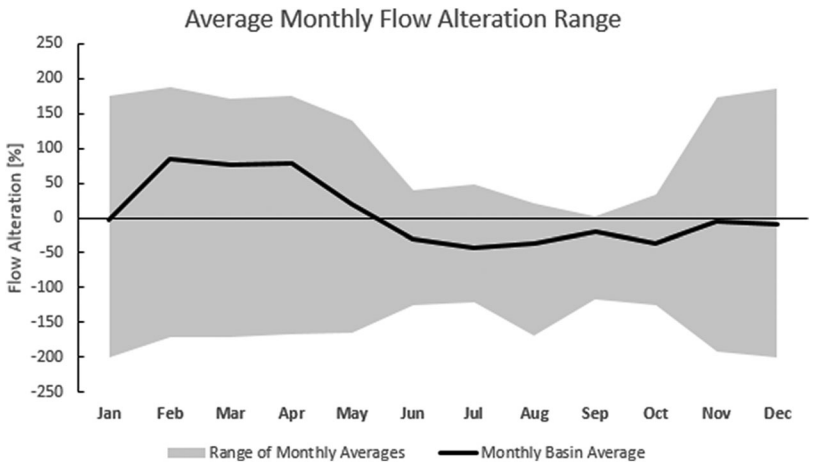

Figure 12. Average monthly flow alteration across basin and range of values from individual reservoirs.

a parcel of water from reservoir entry to exit, it is incapable of estimating residence time of parcels which do not exit reservoirs within the time period. For this reason, reservoirs with higher residence time do not have residence time estimates for the entire time period. While there are some variations among the reservoirs, there are also clear trends. Most reservoirs experience rises in residence time in 2009, 2012, and 2014. Normalizing theses residence times by reservoir averages, averaging across all reservoirs, and plotting with precipitation reveals a possible source of these yearly fluctuations. Figure 11 also shows basin averaged precipitation, revealing a negative relationship between average annual precipitation and basin averaged residence time, where residence time increases when precipitation decreases. Similarly, residence time decreases when precipitation increases. This trend is made evident by a correlation coefficient of -0.65 between annual average precipitation and annual basin-averaged residence time. Logically, when there is more water in the river system, reservoirs typically have higher releases, which lead to lower residence times. Conversely, when there is less water in the river system, inflows and outflows are lower, leading to higher residence time. Additionally, in drier time periods, reservoirs may be operated in such a way to withhold more water than usual to provide additional security in water supply for the uncertain future.

Figure 12 shows the monthly average variation of flow alteration and the range of monthly averages across all reservoirs. This plot highlights the high variability in FA among the reservoirs in the MRB, particularly in transitional months between dry and wet seasons. In November for example, nearly half the reservoirs exhibit high positive FA and the other half exhibit high negative FA. These patterns do not correlate with size, location, or reservoir function, indicating that accurately predicting these alterations is difficult without direct observations of storage change. Figure 13, showing the yearly average FA grouped by overall average FA, exhibits similar variability. While year-to-year variations largely remain consistent for low FA reservoirs, a sharp decrease in FA of all reservoirs with average FA greater than 80% during 2008. The exact cause of this is unknown. Examination of reservoir volume reveals that reservoirs delayed in filling slightly longer in the 2008 wet season than in other years, resulting in part of the wet season flows to release more freely. It is unclear at this time why this trend is only present in the more impactful reservoirs.

One issue associated with the method of filling data gaps using the derived operations curve is that the temporal trends in reservoir storage may be dampened by the temporal trends exhibited by the reservoir operations curve. During larger temporal gaps in useable Landsat images, this would result in the operating policy prescribing its own temporal variability to a time period where the temporal variability is unknown. This is most concerning in the wet season when the number of useable Landsat images is significantly lower (Figure 5). However, based on the results of the Sirindhorn Reservoir (Figure 6), it is only the magnitude of storage that appears erroneous, and not timing, resulting in preserved monthly trends. This mechanism would seek to dampen annual variability, particularly in wet season storage. However, the fact that such drastic annual variability is present in flow alteration and that patterns emerge which appear independent from inflow variations (such as the decrease in annual FA in 2008), suggests that a fair amount of the temporal patterns in storage fluctuation are captured despite potential temporal dampening.

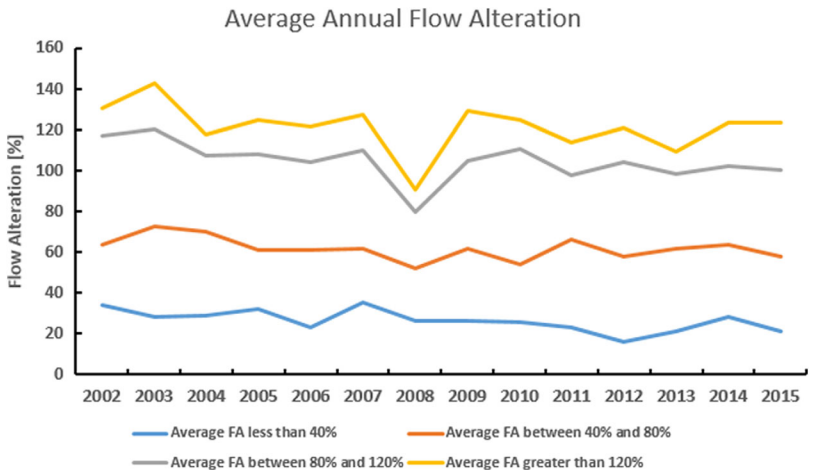

Figure 13. Annual average flow alteration, grouped by flow alteration ranges. Each line represents the average annual FA of all reservoirs with overall average FA within the specified range.

4.2.2. Spatial Variations

Figure 8 qualitatively suggests that reservoir residence time is equally distributed across the basin and there appears to be no correlation between reservoir location and residence time. While this may be the case, the location of the reservoir within the river network plays an important role in the overall effect of the reservoir on basin residence time. Considering the Mekong basin as a whole, the reservoirs studied here caused an average increase in the length of time water spends in the river network by only 3 weeks (0.059 years). When considering only the portion of the overall flow that is regulated by these reservoirs (totaling 17% of basin runoff), the average increase in residence time rises to just over 4 months (0.35 years). Most of the regulated discharge passes through two reservoirs, the Manwan Reservoir on the main stem of the Mekong in China and the Pak Mun Reservoir on the Mun River, a major tributary of the Mekong in Thailand. While neither of these reservoirs is particularly small, they both experience significantly large flows, leading to the extremely short residence times observed in this study. Because of their low residence times, their impact on the overall residence time of the basin is limited. If these dams are excluded, and only regulated discharge from higher-order rivers is considered, the average increase in residence of this discharge becomes 1.3 years. This flow only makes up 3.5% of the total basin discharge, so while these reservoirs have little impact on the basin as a whole, they do have significant impact on local hydrology, specifically, on lower-order streams within the river network. These results are similar to the conclusions drawn by *Grill et al.* [2014], in which the most severe reservoir impacts on streamflow occur in higher tributaries. These impacted waters are diluted as they join flow from unregulated streams, resulting in little impact on the main stem.

Similarly, examining the reservoir's collective impact on MRB outflows at the delta revealed that they have little effect on river basin flow, with an average flow alteration of just 5%. Reducing the scope to only rivers regulated by these reservoirs, the average flow alteration increases to 23%. Removing the Manwan and Pak Mun Reservoirs, which also have the lowest flow alteration, results in an average flow alteration of 89% across the remaining regulated rivers.

The role of stream order is further explored in Figure 14, where residence time is plotted against stream order for the Mekong reservoirs studied here, as well as for all reservoirs in the GRanD database and the average of each stream order. GRanD database reservoir residence time was taken as their DOR expressed in years. Note that there are some reservoirs in the GranD database with residence times higher than 10 years. These were excluded from the plot so that the Mekong reservoirs could be compared with the global situation in better detail. The averages shown include reservoirs beyond the extent of the plot. There is a clear negative trend between residence time and stream order in the global set of reservoirs from GranD, which appears to be mirrored in the Mekong reservoirs. This trend suggests that the most impactful reservoirs in terms of residence time increase tend to be built on lower-order rivers. However, higher-order reservoirs impact a larger amount of flow. As stream order increases, so does river flow and it becomes

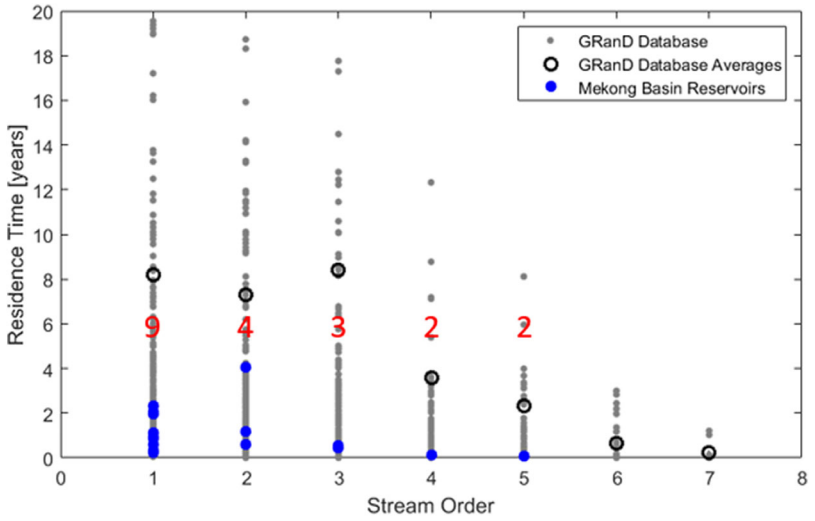

Figure 14. Stream order versus residence time for the MRB reservoirs as well as all GRanD database reservoirs and their averages by stream order. GRanD database residence time taken as the DOR expressed in years. The red numbers signify the number of MRB reservoirs in each stream order.

increasingly difficult or infeasible to build a reservoir that retains water for long periods of time under such high flows. Greater control of smaller flows in lower-order streams can be imposed by smaller reservoirs that can be more feasible to build.

5. Conclusion

This study utilized an array of remote sensing data to observe the operations of reservoirs in the MRB. These reservoir operations were then paired with a hydrologic model and used to derive the impacts these reservoirs have on the streamflow. These impacts were characterized by two parameters: residence time as a measure of how long reservoirs store water, and flow alteration as a measure of the near instantaneous impact on streamflow. Examination of these parameters revealed insightful temporal and spatial patterns. Some patterns are self-evident, such as reservoirs experiencing higher residence time in the dry season than the wet season.

The presence of such an intuitive trend expected of river basins dominated by monsoonal hydrology, adds credibility to the satellite-based method. The fact that satellite observations and physical hydrological model alone are able to elucidate such a trend without any help from in situ observations is notable for ungauged river basins in the developing world. Other less obvious trends provide insights into reservoir operations in the MRB. One such trend is the pattern of highly impactful small reservoirs on smaller tributaries and lower impact larger reservoirs on larger tributaries. Current reservoirs collectively have insignificant impact on the overall MRB system if the MRB is assumed as one single control volume. However, there are two caveats to this "systems" approach. First, the systems approach of a single residence time for the entire basin is valuable for water balance studies only when all riparian nations are working together on a shared vision for integrated water resources management. Second, the single basin-wide metric does not paint the real picture of spatially and temporally diverse human impacts of reservoirs within a basin to identify appropriate and local water management strategies. For example, many reservoirs on lower stream-order rivers have significant impact on the localized streamflow.

Future plans for MRB development involve tripling the number of dams currently in the basin [*International Center for Environmental Management*, 2010]. Basin-wide reservoir impacts on residence time and flow alteration will no longer remain insignificant [*Grill et al*., 2014, 2015]. Another interesting point that emerged is the complete lack of trend in monthly reservoir imposed flow alteration. The fact that no reservoir properties (e.g., size, location, use, etc.) can be used to characterize monthly flow alteration highlights the importance of satellite-based observations to understand how humans operate the reservoirs to maximize benefit.

The key take home message of our study is that satellites can indeed pick out the diverse variability of reservoir operations in ungauged and international river basins that is otherwise intractable. As satellite observations of the water cycle (surface water inundation and height [*Biancamaria et al*., 2016]), precipitation, and soil moisture become increasingly more widespread in the near future, it appears that the scientific community will be able to rely on space observations to understand the potential impact of reservoir development planned by each riparian nation that lacks ground-based observations or data sharing mechanisms. The hope is that the availability of such understanding across a basin will counter the secrecy or the lack of capacity that is typically common among riparian nations of international river basins, and result in a more cooperative environment for the benefit of all the stakeholders of the basin.

Acknowledgments
The authors gratefully express the in situ data obtained from Duc Long of Vietnam National Center for Hydrometeorological Forecasting, Hanoi. Such data were obtained as part of a USAID PEER (Program for Enhanced Engagement in Research) program maintained by the second author with Vietnamese water agencies. This work was partially supported by NASA Applied Sciences grant NNX 15 AC63G under the Water Resources Program and NASA SWOT Science Team grant NNX16AQ54G_9-15-16. Lastly, the authors gratefully acknowledge the guidance received from Hyongki Lee of University of Houston on the use of satellite altimeter data and Gordon Holtgrieve of University of Washington on flow records of the Mekong for calibration of the hydrologic model. Satellite and reservoir data are publicly available but can also be requested by readers to the authors.

References

Adamson, P. T. (2006), Hydrological and water resources modelling in the Mekong Region: A brief overview, in *Mekong Region Waters Dialogue*, IUCN, TEI, IWMI, M-POWER, Vientiane.

Asian Development Bank (ADB) (2004), Cumulative impact analysis and Nam Theun 2 contributions, *Final Rep. E1050*, 143 p., Manila. [Available at http://documents.worldbank.org/curated/en/332511468046791545/Cumulative-impact-analysis-and-Nam-Thuen-2-contributions-final-report.]

Allee, R. J., and J. E. Johnson (1999), Use of satellite imagery to estimate surface chlorophyll a and Secchi disc depth of Bull Shoals Reservoir, Arkansas, USA, *Int. J. Remote Sens.*, *20*(6), 1057–1072.

Ambrosetti, L. Barbanti, and N. Sala (2003), Residence time and physical processes in lakes, *J. Limnol.*, *62*, 1–15.

Beamesderfer, R. C., B. Rieman, L. Bledsoe, and S. Vigg (1990), Management implications of a model of predation by a resident fish on juvenile salmonids migrating through a Columbia River reservoir, *N. Am. J. Fish. Manage.*, *10*(3), 290–304.

Biancamaria, S., D. P. Lettenmaier, and T. Pavelsky (2016), The SWOT mission and its capabilities for land hydrology, *Surv. Geophys.*, *37*(2), 307–337.

Bonnema, M., S. Sikder, Y. Miao, X. Chen, F. Hossain, I. Ara Pervin, S. M. Mahbubur Rahman, and H. Lee (2016), Understanding satellite-based monthly-to-seasonal reservoir outflow estimation as a function of hydrologic controls, *Water Resour. Res.*, *52*, 4095–4115, doi:10.1002/2015WR017830.

Bunn, S., and A. Arthington (2002), Basic principles and ecological consequences of altered flow regimes for aquatic biodiversity, *Environ. Manage.*, *30*, 492–507, doi:10.1007/s00267-002-2737-0.

Crétaux, J. F., and C. Birkett (2006), Lake studies from satellite radar altimetry, *C. R. Geosci.*, *338*(14), 1098–1112.

Costa-Cabral, M. C., J. E. Richey, G. Goteti, D. P. Lettenmaier, C. Feldkotter, and A. Snidvongs (2008), Landscape structure and use, climate, and water movement in the Mekong River basin, *Hydrol. Processes*, *22*(12), 1731–1746.

Döll, P., K. Fiedler, and J. Zhang (2009), Global-scale analysis of river flow alterations due to water withdrawals and reservoirs, *Hydrol. Earth Syst. Sci.*, *13*, 2413–2432, doi:10.5194/hess-13-2413-2009.

FAO/IIASA/ISRIC/ISSCAS/JRC (2012), Harmonized World Soil Database (Version 1.2), Laxenburg, Austria. [Available at http://webarchive.iiasa.ac.at/Research/LUC/External-World-soil-database/HTML/.]

Gao, H. (2015), Satellite remote sensing of large lakes and reservoirs: From elevation and area to storage, *WIREs Water*, *2*(2), 147–157.

Gao, H., C. Birkett, and D. P. Lettenmaier (2012), Global monitoring of large reservoir storage from satellite remote sensing, *Water Resour. Res.*, *48*, W09504, doi:10.1029/2012WR012063.

Gebregiorgis, A. S., and F. Hossain (2014), Making satellite precipitation data work for the developing world, *IEEE Trans. Geosci. Remote Sens.*, *2*, 24–36, doi:10.1109/MGRS.2014.2317561.

Graf, W. L. (2006), Downstream hydrologic and geomorphic effects of large dams on American rivers, *Geomorphology*, *79*(3), 336–360.

Grill, G., C. O. Dallaire, E. Fluet-Chouinard, N. Sindorf, and B. Lehner (2014), Development of new indicators to evaluate river fragmentation and flow regulation at large scales: A case study for the Mekong River Basin, *Ecol. Indic.*, *45*, 148–159, doi:10.1016/j.ecolind.2014.03.026.

Grill, G., B. Lehner, A. E. Lumsdon, G. K. MacDonald, C. Zarfl, and C. R. Liermann (2015), An index-based framework for assessing patterns and trends in river fragmentation and flow regulation by global dams at multiple scales, *Environ. Res. Lett.*, *10*(1), 015001, doi:10.1088/1748-9326/10/1/015001.

International Center for Environmental Management (2010), MRC strategic environmental assessment (SEA) of hydropower on the Mekong mainstream, final report, Mekong River Comm., Hanoi. [Available at www.mrcmekong.org/ish/SEA.htm.]

Ji, L., L. Zhang, and B. Wylie (2009), Analysis of dynamic thresholds for the normalized difference water index, *Photogramm. Eng. Remote Sens.*, *75*(11), 1307–1317.

Johnston, R., and M. Kummu (2012), Water resource models in the Mekong Basin: A review, *Water Resour. Manage.*, *26*, 429–455, doi:10.1007/s11269-011-9925-8.

Keskinen, M., M. Kummu, M. Käkönen, and O. Varis (2012), Mekong at the crossroads: Next steps for impact assessment of large dams, *Ambio*, *41*(3), 319–324, doi:10.1007/s13280-012-0261-x.

Kummu, M., and J. Sarkkula (2008), Impact of the Mekong river flow alteration on the Tonle Sap flood pulse, *Ambio*, *37*, 185–192.

Kummu, M., X. X. Lu, J. J. Wang, and O. Varis (2010), Basin-wide sediment trapping efficiency of emerging reservoirs along the Mekong, *Geomorphology*, *119*(3), 181–197.

Lehner, B., C. R. Liermann, C. Revenga, C. Vörösmarty, B. Fekete, P. Crouzet, and C. Nilsson (2011a), Global Reservoir and Dam (Grand) Database, Version 1, Global Water Syst. Proj. [Available at http://www.gwsp.org/products/grand-database.html.]

Lehner, B., C. R. Liermann, C. Revenga, C. Vörösmarty, B. Fekete, P. Crouzet, and C. Nilsson (2011b), High-resolution mapping of the world's reservoirs and dams for sustainable river-flow management, *Front. Ecol. Environ.*, *9*(9), 494–502.

Liang, X., D. P. Lettenmaier, E. F. Wood, and S. J. Burges (1994), A simple hydrologically based model of land surface water and energy fluxes for general circulation models, *Water Resour. Res.*, *99*(D7), 14,415–14,428.

Ligon, F., W. Dietrich, and W. Trush (1995), Downstream ecological effects of dams, *BioScience*, *45*(3), 183–192.

Lohmann, D., R. Nolte-Holube, and E. Raschke (1996), A large-scale horizontal routing model to be coupled to land surface parametrization schemes, *Tellus, Ser. A*, *48*, 708–721.

Loveland, T. R., B. C. Reed, J. F. Brown, D. O. Ohlen, Z. Zhu, L. Yang, and J. W. Merchant (2000), Development of a global land cover characteristics database and IGBP DISCover from 1 km AVHRR data, *Int. J. Remote Sens.*, *21*(6–7), 1303–1330.

McFeeters, S. K. (1996), The use of the normalized difference water index (NDWI) in the delineation of open water features, *Int. J. Remote Sens.*, *17*(7), 1425–1432.
McGuire, M., A. W. Wood, A. F. Hamlet, and D. P. Lettenmaier (2006), Use of satellite data for streamflow and reservoir storage forecasts in the Snake River Basin, *J. Water Resour. Plann. Manage.*, *132*(2), 97–110.
Mekong River Commission (MRC) (2011), Assessment of basin-wide development scenarios, main report, Vientiane. [Available at http://www.mrcmekong.org/assets/Publications/basin-reports/BDP-Assessment-of-Basin-wide-Dev-Scenarios-2011.pdf.]
Monsen, N. E., J. E. Cloern, L. V. Lucas, and S. G. Monismith (2002), A comment on the use of flushing time, residence time, and age as transport time scales, *Limnol. Oceanogr.*, *47*(5), 1545–1553.
Poff, N. L., and J. K. H. Zimmerman (2010), Ecological responses to altered flow regimes: A literature review to inform the science and management of environmental flows, *Freshwater Biol.*, *55*, 194–205, doi:10.1111/j.1365-2427.2009.02272.x.
Pringle, C. (2003), What is hydrologic connectivity and why is it ecologically important?, *Hydrol. Processes*, *17*(13), 2685–2689, doi:10.1002/hyp.5145.
Rueda, F., E. Moreno-Ostos, and J. Armengol (2006), The residence time of river water in reservoirs, *Ecol. Modell.*, *191*(2), 260–274.
Schmutz, S., and C. Mielach (2015), Review of existing research on fish passage through large dams and its applicability to Mekong mainstream dams, *Tech. Pap. 48*, p. 149, Mekong River Comm., Phnom Penh.
Seeber, C., H. Hartmann, and L. King (2010), Land use change and causes in the Xiangxi catchment, Three Gorges Area derived from multispectral data, *J. Earth Sci.*, *21*(6), 846–855.
Thanapakpawin, P., J. Richey, D. Thomas, S. Rodda, B. Campbell, and M. Logsdon (2007), Effects of landuse change on the hydrologic regime of the Mae Chaem river basin, NW Thailand, *J. Hydrol.*, *334*(1), 215–230.
Vörösmarty, C. J., M. Meybeck, B. Fekete, K. Sharma, P. Green, and J. P. Syvitski (2003), Anthropogenic sediment retention: Major global impact from registered river impoundments, *Global Planet. Change*, *39*(1), 169–190.
Vörösmarty, C. J., K. P. Sharma, B. M. Fekete, A. H. Coperland, J. Holden, J. Marble, and J. A. Lough (1997), The storage and aging of continental runoff in large reservoir systems of the world, *Ambio*, *26*, 210–219.
Winemiller, K. O., et al. (2016), Balancing hydropower and biodiversity in the Amazon, Congo, and Mekong, *Science*, *351*(6269), 128–129, doi:10.1126/science.aac7082.
Yoon, Y., and E. Beighley (2015), Simulating streamflow on regulated rivers using characteristic reservoir storage patterns derived from synthetic remote sensing data, *Hydrol. Processes*, *29*, 2014–2026, doi:10.1002/hyp.10342.
Zarfl, C., A. E. Lumsdon, J. Berlekamp, L. Tydecks, and K. Tockner (2015), A global boom in hydropower dam construction, *Aquat. Sci.*, *77*(1), 161–170.